The Si vacancy: an example of a pressure-sensitive Jahn-Teller system

1993 J. Phys.: Condens. Matter 5 1863

(http://iopscience.iop.org/0953-8984/5/12/013)

J. Phys.: Condens. Matter 5 (1993) 1863–1876. Printed in the UK

The Si vacancy: an example of a pressure-sensitive Jahn–Teller system

Eugen Tarnow†
2124 Rock Street, #45, Mountainview, CA 94043, USA

Received 26 October 1992

Abstract. We calculate the trends in the Jahn–Teller (JT) parameters of the Si vacancy as a function of the breathing mode coordinate. Using *ab initio* local-density-functional theory we find the couplings between the JT modes and the breathing mode to be significant. Since the breathing mode coordinate is very sensitive to pressure we predict a pressure-sensitive JT contribution to the effective electronic correlation energy U. Furthermore we find that the tetragonal JT energy increasingly dominates over the trigonal energy as the pressure increases due to a softening of the tetragonal spring constant. We introduce an approximation to deal with the spurious supercell-induced dispersion and splittings.

1. Background

The Jahn–Teller (JT) and quasi-JT systems make up a peculiar class of point defects. In these a symmetry breaking occurs for a charge state in which a degenerate or quasi-degenerate set of localized electronic levels is partially occupied [1]. One of the simplest such defects is the Si vacancy which has served for many years as a prototypic JT system to study. In this contribution we extend previous work on the JT properties of the vacancy to include effects of pressure [2]. Readers who are familiar with the Si vacancy and are not interested in the details of our calculations may skip to section 5.

Let us review some relevant facts about the Si vacancy (for a thorough review see [3] and [4]) using the one-electron picture, which experiment finds to be accurate [3].

It is known that the four Si dangling-bond orbitals combine to form a filled a_1 symmetric state in the valence band and a triply degenerate state of t_2 symmetry in the fundamental gap. When filling the latter states, a JT distortion occurs. There are twelve distortions possible for the vacancy nearest neighbours (we will consider only these *local* distortions, similar to Messmer and Watkins [5]). Six of these correspond to overall translations and rotations and need not be considered (these only change the relationship between first- and second-nearest neighbours, which we also do not consider in the local approximation). The others are a breathing mode, two degenerate tetragonal distortions and three degenerate trigonal distortions. The trigonal and tetragonal distortions break the T_D symmetry. This gives us an electronic

† Present address: Electronic Research Group, Los Alamos National Laboratory, MS D429, Los Alamos, NM 87545, USA. Email: Tarnow@Netcom.com.us.

0953-8984/93/121863+14$07.50

energy change which is linear in the distortion, while the energy cost from the lattice is quadratic in the distortion. The Hamiltonian is usually written

$$H = kx^2/2 + nVx \tag{1}$$

where k is the mode spring constant, x is the distortion, V is the JT potential and n (= 0, 1, 2) is the number of electrons in the symmetry-broken state. The Hamiltonian is minimized at $x = -nV/k$ with a minimum energy of

$$E_{\min} = -(nV)^2/2k. \tag{2}$$

The JT contribution to the effective electronic correlation energy U_{eff} is

$$U_{\text{JT}} = E_{\min}(n = 0) + E_{\min}(n = 2) - 2E_{\min}(n = 1) = -V^2/k. \tag{3}$$

This contribution was predicted to possibly lead to an overall negative effective correlation energy [6] and this is consistent with experimental data [3].

There are at least two problems open to pursue for the Si vacancy:

(i) Experiment finds the tetragonal symmetry breaking to be dominant at zero pressure [3]. Even though theory has confirmed this result for the singly negative charge state in a symmetry-unrestricted optimization [7], the JT parameters for the alternative trigonal distortion remain to be calculated.

(ii) We need to study the behaviour of the coupling of the JT parameters to other modes in the solid. The general situation of a coupling of the JT coefficients to quadratic modes was investigated by Leihr and Ballhausen in 1957 [8]. In the theoretical literature on the Si vacancy there is mentioned a variation of the tetragonal JT parameter with the breathing mode [4, 9–11], but this result is only commented on superficially [12–15]. Messmer and Watkins presented a more detailed picture in an extended Huckel theory calculation on the vacancy in diamond [16].

In this paper we will attack the coupled JT problem for both tetragonal and trigonal distortions. We calculate trends of all JT parameters using *ab initio* local-density-functional theory. We deal with the artificial supercell-induced dispersion and splitting of the JT levels by introducing what we call 'the degenerate k-point approximation' (DkA).

The organization of this paper is as follows. In section 2 we discuss the computational method. We give results regarding the symmetric configuration in section 3. In section 4 we apply a correction to our raw data according to the DkA. In sections 5 and 6 we investigate the symmetry-breaking tetragonal and trigonal parameters, respectively. In section 7 we compare the JT energies of these two distortions. Section 8 examines the effects of a coupled JT system and section 9 concludes the paper.

2. Calculational details and the degenerate k-point approximation

The computations were performed within the framework of density-functional theory using the local-density approximation (LDA) combined with Hamann–Schluter–Chiang

pseudo-potentials (and a matrix diagonalization program) and Kleiman–Bylander pseudo-potentials (and a conjugate gradient program) and the supercell method [17]. A 7 Ryd plane wave cutoff was utilized (we tested our results up to 11 Ryd), and the supercell lattice constant was frozen at the experimental value. Our calculations were performed in supercells with 32 and 64 atoms. The breathing and JT distortions of the vacancy nearest neighbours were fixed. The other atoms were relaxed until the corresponding forces were less than 0.1 eV $Å^{-1}$/atom. The JT potential was calculated by taking $\frac{2}{3}$ of the electronic level splitting and dividing by the distorting distance (about 0.25 Å). The spring constants were calculated from the energy differences of the distorted and undistorted states. All JT parameter calculations were performed in the doubly positive charge state.

In the supercell approximation, two spurious effects make it difficult to extract the JT parameters. First, the periodicity introduces an artificial dispersion of the degenerate JT states (0.5–1.0 eV in supercells of 32–64 atoms). This destroys the JT effect and makes it, at best, a pseudo-JT effect, second, a 'supercell material' (in our case, the crystal unit cell consists of N Si atoms and a vacancy) has symmetry-lowering-induced electronic splittings of its own (analogous to strain-induced band splittings) that interfere with the local JT effect.

There are at least two ways to deal with these obstacles. One way is to try to filter out these effects using a simpler model calculation [18]. This is, however, usually not *ab initio* and the dispersion from the simpler model may be different from the dispersion of the LDA calculation. In this paper we introduce a second alternative which we call the 'degenerate k-point approximation' (DkA). This is a substantial improvement over the procedure in, for example, [7] in which the spurious supercell-induced effects were not considered.

There are two features to the DkA. Firstly, we perform our calculations at k-points for which the JT relevant undistorted states (for example, the t_2 states of the Si vacancy) are degenerate. This allows us to see the degeneracy lifted by an amount linear in the symmetry breaking JT distortions. Secondly, if we want to obtain the pure JT effect, we need to understand and separate out the 'supercell material' symmetry-lowering-induced contribution to the splittings.

Let us first discuss the case of the supercell being cubic. Then the little group of the degenerate k-point turns out to be T_d, which is the same as the point group of the vacancy. Thus the electronic bands fall in the same pattern of representations as would the states of the truly isolated vacancy. In particular, the true vacancy t_2 states form a three-dimensional representation. In the supercell approximation, extended parts are added to these states and the final extended wavefunctions, at the degenerate k-point, also form a three-dimensional representation. Because of the equivalent symmetry groups, the splittings induced by the symmetry breaking will divide the representations into identical collections of smaller representations. For example, tetragonal and trigonal symmetry breakings will divide the three degenerate states into a singlet and a doublet, both for the true vacancy states and for the extended supercell states.

If the supercell is not cubic, and the periodic arrangement of the vacancies has a symmetry lower than T_d, the symmetry groups will no longer be equivalent. Thus the bands at the degenerate k-point may only be accidentally degenerate and the splittings induced by the symmetry breaking will divide the representations into potentially *different* collections of smaller representations. To study the JT effect under these conditions, it is most convenient to pick a JT distortion that keeps the dimensionality

of the broken point group as high as possible, i.e. for the 32-atom cell, we need to choose one of the trigonal distortions. If we use the one directed along the C_{3v} axis of symmetry, the triply (accidentally) degenerate states split into a doublet and a singlet, just as for the trigonal distortion of the vacancy. If we used another trigonal distortion, the symmetry of the unit cell would be lowered and we would obtain three different singlet states.

The 'supercell material' and JT effects can be approximately separated since they act differently as a function of the breathing mode. While the extended effects are relatively insensitive to changes in the local breathing mode (corresponding to small changes relative to the size of the unit cell), the local JT effect is very sensitive (corresponding to changes comparable to the size of the vacancy). As we separate the atoms from each other, the local JT effect disappears, leaving us with the pure 'supercell material' symmetry breaking. After performing a calculation for large breathing modes we then subtract the effects of the 'supercell material' symmetry breaking and end up with the true local JT parameters.

For each individual calculation one degenerate k-point is used. We will study the quality of the DkA by using two different supercells, of 32 and 64 atoms, and two different degenerate k-points for each supercell. We hope to show that consistent results can be obtained already with our 32–64 atom unit cells. (As the size of the unit cell goes to infinity the approximation becomes exact, of course.) Thus for the 32-atom cell, the (0.25, 0.25, 0.25), in units of reciprocal lattice vectors (S(32), for short), and Γ ($\Gamma(32)$) points were used which gave gap states degenerate to within 0.02 eV and 0 eV, respectively (the former dividing into one singlet and one doublet from the C_{3v} symmetry of the little group). This is in contrast with the t_2 dispersion of a general k-point of 0.5–1.0 eV. For the 64-atom cell the (0.5, 0.5, 0.5) (T(64), for short) and Γ ($\Gamma(64)$) points were used both with completely degenerate t_2 states (both have little groups of T_d symmetry).

This work represents one of the first occasions that the supercell method has been applied to study properties of the symmetry breaking of degenerate point-defect states [18, 19].

3. Results of symmetric geometries

3.1. The breathing mode

Let us study the structural quality of the DkA and calculate the breathing mode coordinate and spring constant. Previous work indicates that the breathing mode coordinate minimum is controversial [20–22]. Baraff *et al* [9] find a spring constant of 7.5 eV Å^{-2} while Larkins and Stoneham [23] give a value of 4.0 eV Å^{-2}, both groups using valence force fields. Scheffler *et al* [24] give a value of 29 ± 12 eV Å^{-2} and experimental estimates by DeLeo *et al* [25] give 20 and 27 eV Å^{-2}. We calculated the energy of the +2 state as a function of the breathing mode coordinate and the results from the four calculations are shown in table 1. We find a spread of energy minima from 2.20 to 2.57 Å, and a spread in spring constants from 3.2 to 9.9 eV Å^{-2}. If we average the four values with equal weight we find the energy minimum at 2.4 ± 0.2 Å and a spring constant of 7 ± 3 eV Å^{-2} [26, 27].

Although we cannot state whether the +2 charge state expands or contracts the lattice, the *difference* in size as a function of pressure should be more accurate due to

Table 1. Breathing mode coordinate and spring constant for different degenerate k-points.

k-point	B_{min} (Å)	k_B (eV Å^{-2})
Γ(32)	2.20	3.2
S(32)	2.45	8.6
Γ(64)	2.56	5.6
T(64)	2.57	9.9

cancellation of errors. Using the T(64) point we calculated the change in the value of the breathing mode coordinate B as we imposed pressure by changing the size of the unit cell. A 5% decrease in the size of the unit cell resulted in a 19% decrease in B. This gives us a displacement ratio of about four which supports an earlier finding that B is very sensitive to pressure [28]. In addition we notice the curious fact that the bonds of the vacancy's nearest-neighbour atoms are able to extend and contract by a large amount (for example, at $B = 2.53$ Å these bonds have stretched by 8%).

3.2. Electronic states

While there is no experimental measurement of the optical transition energy of the t_2 states, theory generally places the states near mid-gap (see, for example, [9]). We find some discrepancies between the different degenerate k-points: the t_2 states lie at different points in the gap in the different calculations. Thus the S(32) and T(64) points have t_2 states about 1 eV separated from the extended states above and below, while both Γ points have t_2 states only 0.18 eV away from the lowest conduction band state. This allows the t_2 states at Γ to mix with the conduction bands and lose some lone-pair character. Indeed, the t_2 states at Γ(32) are less localized on the four vacancy neighbours than those at S(32) (35% and 49%, respectively, by integrating the charge around the atoms). Furthermore, at Γ(32) there are three states appearing above the bottom of the conduction band that are also degenerate and also have a significant charge density on the vacancy neighbours, another sign of mixing of the t_2 levels with the conduction bands.

Finally, we plot the energy change of the t_2 states as a function of B in figure 1, which should be accurate due to error cancellation. Indeed, our values are in good agreement with those of [9] and [10] as shown, and [24] and [31] (not shown). Consistent with this result, B decreases by 0.3 Å as we completely fill up the t_2 states (charge state −4) for the S(32)-point calculation [32]. Note that the B deformation potential (the derivative of the energy w/r to the breathing coordinate) seems to go through a maximum around 2.4 Å.

4. Raw data and the separation of the local JT contribution

From our calculations at different degenerate k-points we obtain the combined JT and extended-state energy splittings as a function of the breathing coordinate B, shown in figures 2 and 3. We notice that all curves give consistent trends for small B. This shows that we obtain consistent results for the k-point-independent local JT effect.

The curves are offset from each other by different amounts resulting from different wave functions extending between the periodically repeated vacancies. To get the true

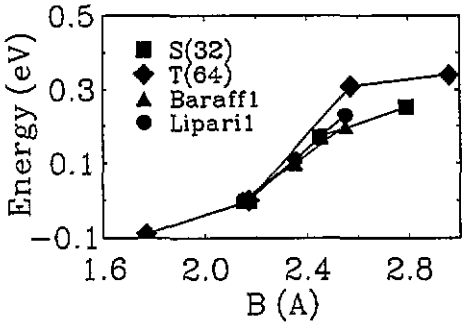

Figure 1. Energy change of t_2 states as a function of B. Note that we have arbitrarily set the energy to 0 eV at 2.15 Å.

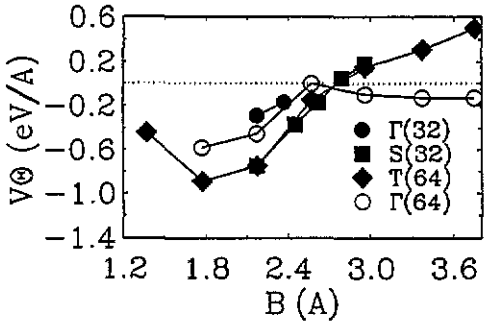

Figure 2. Raw data of V_Θ as a function of the breathing mode coordinate B.

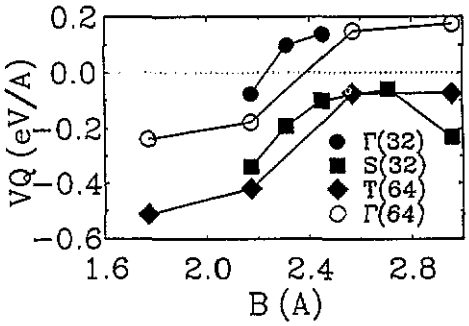

Figure 3. Raw data of V_Q as a function of the breathing mode coordinate B.

JT splittings we should subtract the contribution of the splitting at large B. For the trigonal distortion, this operation is simple, since the splittings in the large unit cell become constant. We perform this operation for the data from the T(64) calculation and we obtain our prediction for the trigonal JT potential shown in figure 5.

For the tetragonal distortion, the large-B splittings keep changing rather than becoming constant. Thus it is now much harder to separate the JT symmetry breaking from the supercell symmetry breaking. We content ourselves with a two-parameter fit to the splittings at large B values. We fit these from the data at 3.0 Å and above. The correction we obtain is rather large (about 0.5 eV for the largest and smallest values of B). The result of the separated tetragonal JT potential is shown in figure 4.

5. Tetragonal JT parameters

We considered the energy parameters associated with the tetragonal (Θ) and trigonal (Q) modes of symmetry breaking. The notation and coordinates of these displacements have been given elsewhere [5]. All calculations were performed in the

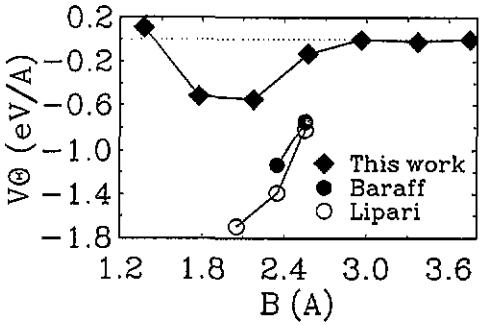

Figure 4. Corrected V_Θ as a function of the breathing mode coordinate B.

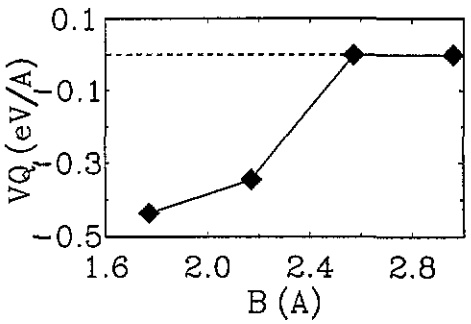

Figure 5. Corrected V_Q as a function of the breathing mode coordinate B.

+2 charge state, for which there are no electrons in the degenerate electronic states. Let us begin by considering the Θ mode.

Earlier calculations by Baraff *et al* [9] give $k_\Theta = 3.7$ eV Å^{-2} and $V_\Theta = -1.12$ eV Å^{-1} (the latter value for $B = 2.35$ Å; for $B = 2.55$ Å we calculate $V_\Theta = -0.76$ eV Å^{-1} from their data). The sign indicates that for a positive distortion, defined as a pairing [9], a single electronic state referred to as B_2 moves down and two E states move up. Conflicting values of $V_\Theta = -4$ and -0.5 eV Å^{-1} are given by Kirton *et al* [11, 33], and of $V_\Theta = -0.3$ and -8 eV Å^{-1} by Jaros *et al* [31, 34]. From Kelly *et al* [20] we calculate $k_\Theta = 2.8$ eV Å^{-2} and abs(V_Θ) $= 0.79$ eV Å^{-1} at $B = 2.15$ Å. From Lipari *et al* [10] we calculate values of $V_\Theta = -1.70$, -1.39 and -0.82 eV Å^{-1} at $B = 2.05$, 2.35 and 2.55 Å, respectively. Experimental estimates for k_Θ are 1.7 and 1.3 eV Å^{-2} [25]. A simple central-force model gives $k_\Theta = 11.9$ eV Å^{-2} [30, 35]. A semi-empirical calculation of the vacancy in diamond shows a strong dependence of the JT potentials on the breathing mode coordinate [16].

Our results for k_Θ and V_Θ as a function of the breathing coordinate B are shown in figures 6 and 4, respectively. We see that k_Θ increases with the breathing coordinate. This is consistent with the Θ distortion becoming more difficult as the increasingly planar sp^2-hybridized geometry prevents the in-plane Θ distortion. Notice the anomalous small value of k_Θ at $B = 1.77$ Å. It is presumably a result of the failure of the vacancy's second-nearest-neighbour atoms to respond to the breathing distortion. This gives rise to bonds to the nearest neighbours that have been stretched by 8% to 2.53 Å, and thereby considerably weakened. This result could not have been arrived at using the simple Keating force model of [9].

For B of about 2.4 Å, V_Θ decreases with the breathing coordinate. As we see, the calculations in [9] and [10] also suggest a similar dependence [13, 14]. Interestingly, for very small B, V_Θ levels off and decreases. This may be due to the electronic states having a certain minimal spacial extent from minimizing the kinetic energy, and as the atoms move closer and closer, the wavefunctions cease to respond to the symmetry-breaking movements of the vacancy's neighbours. As stated above, we noticed a similar behaviour of the deformation potential that seemed to have a maximum around $B = 2.4$ Å, which is where we also see the largest derivative in V_Θ [36].

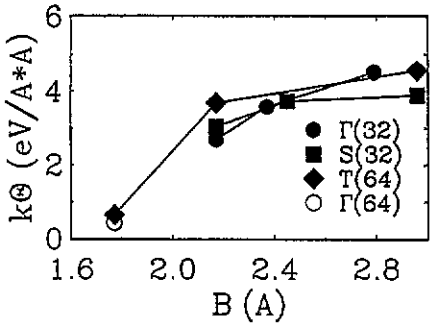

Figure 6. k_Θ as a function of the breathing mode coordinate B.

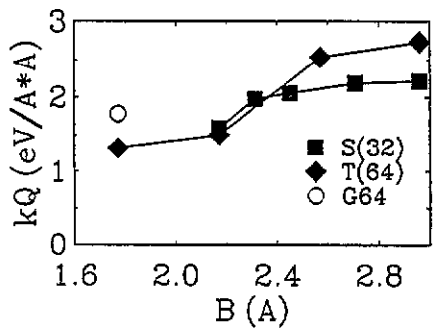

Figure 7. k_Q as a function of the breathing mode coordinate B.

Our charge densities are similar to earlier work (see, for example, [9]). As found in [7], the intercellular overlap along the [110] direction is significant.

Our error analysis cannot identify the source of discrepancy with the data in [9] and [10] (see [37]). The effects of our finite supercell size seem small, and will no doubt soon be made even smaller with use of the new parallel algorithms that allow for larger supercells [38]. A parallel calculation is especially simple to perform since V_Θ is almost independent of relaxations away from the nearest neighbour Si atoms and forces would not need to be calculated [37].

6. Trigonal JT parameters

Earlier calculations of the trigonal JT potential give the value abs(V_Q) = 4.5 eV Å^{-1} [11] (the sign convention is not clear). A simple nearest-neighbour central-force model gives k_Q = 5.95 eV Å^{-2} [30,35], and a large-cluster valence-force model gives k_Q = 0.97 eV Å^{-2} [30,39]. A Keating model gives k_Q = 1.82 and 3.62 eV Å^{-2} for two different trigonal distortions [9,40]. It is customary to consider the ratio k_Q/k_Θ: for a central force model, in which the only atoms moved are the vacancy's nearest neighbours, and for which the equilibrium B value is taken to be the Si–Si bond length, the ratio of the force constants is exactly 0.5 [30,35].

Our results for k_Q and V_Q are shown in figures 7 and 5, respectively. We find that the ratio of k_Q/k_Θ is somewhat smaller than 0.5 near 2.35 Å, and it decreases for smaller B. Abs(V_Q) increases as we lower B, as does V_Θ.

In the trigonal distortion considered one atom moves straight out from the vacancy while the three other atoms move closer to (but not straight to) the centre. The charge densities show that the singlet state consists primarily of a lone pair on the atom that moves outwards. The movement causes an increase in sp^2 hybridization that increases the relative s content of the state and therefore lowers its energy.

This 'model' predicts that the trigonal JT potential should be negative until the breathing mode is so large that it forces the vacancy's neighbours to have their three bonds in a plane. If the dangling bonds are still interacting, further increasing the breathing mode coordinate would *decrease* the sp^2 hybridization and thus change the sign of the trigonal JT potential. A sign change is seen in earlier semi-empirical

calculations in diamond, but it takes place at too low a value of the breathing coordinate to be consistent with our model [16].

7. Calculated JT energies

U_{JT}, the JT contribution to the effective electronic correlation energy U_{eff} (see section 1), is shown in figure 8 for the tetragonal and trigonal modes. Both values of U_{JT} are largest at small values of B. The two energies are similar around $B = 2.4$ Å, which is consistent with experiment [3]. For smaller B, the tetragonal energy comes to dominate [41].

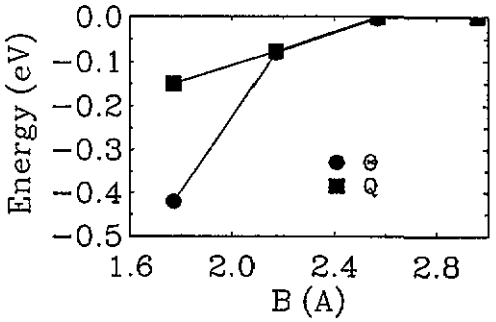

Figure 8. Calculated values of the JT contribution to the effective electronic correlation energy, $U_{JT} = -V^2/k$.

From figure 8 we find that the tetragonal JT energy for small B can be quite large. If we lower the lattice constant of the sample by up to about 10% (corresponding to a pressure of about 125 kBar), at which point Si takes a complete β-tin structure [42], then the corresponding breathing mode coordinate would decrease by about 40% (0.9 Å). Thus we could reach JT energies of 0.5 eV. At this point, the split B_2 state with two electrons has moved down by $-2V^2/k$ or $-2U_{JT}$ eV and the E states have moved up by U_{JT} eV. Thus both states have left the gap. Finally, the barrier for reorientation from one broken-symmetry configuration to another is $U_{Re} = 0.75(E_\Theta - E_Q)$ [3]. For small B this difference increases and we predict the reorientation should become more difficult.

In [9] the effect on the effective electronic correlation energy U_{eff} from the B deformation potential was calculated:

$$E_{DP} = -nV_{DP}^2/2k_B \tag{4}$$

and

$$U_{DP} = -V_{DP}^2/k_B \tag{5}$$

where E_{DP} and U_{DP} are the B deformation potential energy and contribution to U_{eff}, respectively, V_{DP} is the B deformation potential and k_B is the breathing mode spring constant. These authors found that U_{DP} was rather small, only about 0.02 eV. Thus we do not further consider this correction.

Finally, let us consider the effects of the JT symmetry lowering on the different charge states. Experimentally the tetragonal energy dominates for the +1 and 0 states. The trigonal distortion becomes secondary and only occurs for the singly negative charge state [3, 43]. The symmetry lowerings of the states with more electrons can be thought of in terms of an electron–hole symmetry that takes t_2 states with N electrons and maps them onto t_2 states with N holes. Thus the (-2) charge state, which has 2 holes in the t_2 states, is mapped onto the neutral state which has 2 electrons. It should therefore undergo a pure tetragonal distortion [43]. If we continue to fill up the t_2 states the -3 state should undergo a smaller tetragonal distortion and the -4 state should have full T_D symmetry. The high-occupancy -4, -3 and -2 charge states should have a large U_{JT} associated with them, just as the $+2$, $+1$ and 0 states do. In fact, because of the decrease in B as we add electrons, the U_{JT} for the -4, -3 and -2 states should be the larger [44].

8. Discussion of the coupled JT system

Leihr and Ballhausen [8] considered the effects of coupling the JT distorting modes to other modes in a doubly degenerate system. Here we summarize (and simplify somewhat) the case of a degenerate system for which the JT distortion is coupled to a symmetric breathing distortion.

The Hamiltonian for this system, up to second order in x and B is (while neglecting the coupling between B and the electronic occupation as before)

$$H = kx^2/2 + k_B(B - B_0)^2/2 + nVx + n\Gamma xB \tag{6}$$

where k and V are the JT parameters, k_B is the B-mode spring constant, n is the number of electrons in the JT state and Γ is the coupling between the JT and B modes. The breathing coordinate minimum is at $B = B_0$ for $n = 0$. Let us integrate out the breathing mode coordinate by setting its derivative to be zero, i.e.

$$B - B_0 = -n\Gamma x/k_B. \tag{7}$$

The new Hamiltonian we obtain is

$$H' = 0.5kx^2(1 - n^2\epsilon) + nVx \tag{8}$$

where

$$\epsilon = \Gamma^2/2kq. \tag{9}$$

The new breathing-mode coordinate is

$$B - B_0 = (n\Gamma nV/k)/[(1 - n^2\epsilon)/q] = 2n^2\epsilon(V/\Gamma)/(1 - n^2\epsilon).$$

The effect of the coupling is accordingly to shift the breathing-mode coordinate away from B_0 and to soften the effective spring constant of the mode x by the factor $(1 - n^2\epsilon)$. Note that dependence upon the occupation factor n makes these effects largest in the doubly occupied state. Interestingly, if the coupling Γ is large enough the Hamiltonian starts to diverge and the quadratic approximation fails. In this case one could obtain two sets of JT metastable states [8].

The negative effective electronic correlation energy is enhanced by the coupling Γ. To first order in ϵ,

$$U_{JT} = -(V^2/k)(1 + 7\epsilon). \tag{10}$$

Let us calculate the correction factor for the Si vacancy and the tetragonal state. We use the following parameters: $\Gamma = 0.6$ eV Å^{-2}; $k = 4$ eV Å^{-2}; $q = 10$ eV Å^{-2}; and obtain $\epsilon = 0.004$. Accordingly, we have the case for which the Hamiltonian (6) is stable. U_{JT} is enhanced by only 3%.

Thus we find that while the pressure-induced effects of the JT coupling to B are large (see section 7), the 'internal' effects are small.

9. Conclusion

The JT potential coupling to the breathing mode has several consequences for the Si vacancy. We predict that increasing the pressure will significantly increase the size of U_{JT}, as will increasing the charge on the vacancy. U_{JT} of the -4, -3 and -2 charge state combination of the Si vacancy would be larger than for the known $+2$, $+1$ and neutral charge state combination. These highly negative charge states may possibly be realized if there is a charge-compensating weakly interacting impurity present. Differently sized vacancy-like substitutional impurities should show size-dependent JT energies [45]. The reorientation energy from one symmetry-broken state to another should increase for sufficiently large pressures. The 'internal' effects (previous section) of the coupling were however small, only amounting to a change in U_{JT} of a few percent. Finally, the sensitivity of the breathing mode coordinate to pressure indicates a sensitivity of the bond lengths and bond strengths of the three back bonds to the vacancy's nearest neighbours. This gives us a model system for which we easily can manipulate bond strengths.

Other potentially similar systems include the Si (100) surface which has quasi-JT distorting dangling bonds. The symmetry breaking is shown in the tilting of the dimer bonds and this tilt angle should be sensitive to pressure changes. Other Peierls distorting systems like polyacetylene should show pressure dependencies. Also, while the JT effects of the Si divacancy seem to be small at zero pressure [46], they may become more substantial under pressure. We would expect the JT potentials of these and other JT systems to first increase and then decrease with pressure.

Finally, one should investigate other JT systems to get an overall picture of the importance of JT couplings to other modes, and to see whether this coupling is always small or whether it can be as large as to change the stability of the JT distortion (see section 8).

Acknowledgments

I am grateful to Dr T Arias and Professor J D Joannopoulos for giving me the computer codes. Critical readings by Dr M Needels and Professor G Watkins are acknowledged. This work was in part supported by the Office of Naval Research through Contract no N00014-82-C-0244.

References

[1] Jahn H A and Teller E 1937 *Proc. R. Soc.* A **161** 220

[2] A study of vacancy diffusion under pressure was performed by Antonelli A and Bernholc J 1989 *Phys. Rev.* B **40** 10643

[3] Watkins G D 1986 *Deep Centers in Semiconductors* ed S T Pantelides (New York: Gordon and Breach) p 147

[4] Stoneham A M 1975 *Theory of Defects in Solids* (Oxford: Clarendon) ch 27

[5] Messmer R P and Watkins G D 1973 *Phys. Rev.* B 7 2568. Our trigonal Q mode is their Q_a mode. Note that we give the coordinates of the symmetry lowering modes in terms of normal coordinates, while we leave the breathing mode as the real distance to the vacancy centre.

[6] Baraff G A, Kane E O and Schluter M 1979 *Phys. Rev. Lett.* **43** 956

[7] Sugino O and Oshiyama A 1992 *Phys. Rev. Lett.* **68** 1858

[8] Leihr A D and Ballhausen C J 1957 *Ann. Phys.* **3** 304

[9] Baraff G A, Kane E O and Schlüter M 1980 *Phys. Rev.* B **21** 5662

[10] Lipari N O, Bernholc J and Pantelides S T 1979 *Phys. Rev. Lett.* **18** 1354

[11] Kirton M J, Banks P W, Lian Lu Da and Jaros M 1984 *J. Phys. C: Solid State Phys.* **17** 2487

[12] Stoneham ([4] p 874) writes that in the diamond lattice 'if the totally symmetric forces are indeed as large as indicated, then non-linear terms proportional to $Q_A Q_\Gamma$ ($B\Theta$ or BQ in our notation) cannot be ignored'.

[13] That there is a dependence of V_Θ upon the breathing coordinate could be calculated from the results in [9]. No explicit mention of this dependence was made, and it was not included in the error analysis at the end of the paper.

[14] From [10] one can calculate a dependence. These authors' comment on the dependence of V_Θ upon the breathing coordinate is that 'the calculations indicate that a combination of tetragonal and breathing displacements can indeed place the energy level of the fully occupied doublet in the lower part of the gap, as found experimentally'.

[15] The ratio of k_Q/k_Θ can change as the breathing mode changes, according to [11].

[16] Messmer R P and Watkins G D 1971 *Radiation Effects in Semiconductors* ed J W Corbett and G D Watkins (London: Gordon and Breach) p 9

[17] For a review article covering the computational procedures used see
Payne M C, Teter M P, Allan D C, Arias T and Joannopoulos J D 1992 *Rev. Mod. Phys.* **64**

[18] A supercell method with a dispersion-compensating simple tight-binding model was introduced in
Louie S G, Schlüter M, Chelikowski J R and Cohen M L 1976 *Phys. Rev.* B **13** 1654
The authors calculated the average position of the degenerate t_2 states for the vacancy, but failed to correctly reproduce the tetragonal JT effects. Thus for both negative and positive symmetry-lowering distortions exactly one vacancy level is split away to lower energies (the JT effect should be anti-symmetric with one vacancy level lowered and two levels increased for one type of distortion, and one level increased and two levels lowered for the opposite distortion).

[19] The first supercell calculation was probably done by
Messmer R P and Watkins G D 1973 *Radiation Damage and Defects in Semiconductors 1973 (Inst. Phys. Conf. Proc. 16)* ed J E Whitehouse (London: Institute of Physics) p 255
These authors noted the large dispersion of the vacancy defect levels in a 64-atom diamond unit cell.

[20] Kelly P J, Car R and Pantelides S T 1986 *Defects in Semiconductors (Materials Science Forum)* vol 10–12, ed H J von Bardeleben (Aedermannsdorf: Trans Tech) p 115

[21] Kelly P J and Car R 1992 *Phys. Rev.* B **45** 6543

[22] Samara G A 1988 *Phys. Rev.* B **37** 8523

[23] Larkins F P and Stoneham A M 1971 *J. Phys. C: Solid State Phys.* 4 143
[24] Scheffler M, Vigneron J P and Bachelet G B 1985 *Phys. Rev.* B 31 6541
[25] DeLeo G G, Fowler W B and Watkins G D 1984 *Phys. Rev.* B 29 3193
[26] As we will see later, the breathing mode is very sensitive to pressure and therefore to the lattice constant. Because the relaxed lattice constant (as opposed to the frozen lattice constant used in our calculation) varies somewhat with cutoff energy, we see a spurious variation in pressure. Accordingly, our results with regard to the breathing mode coordinate minimum are not conclusive. The breathing mode spring constant should be less sensitive to this effect.
[27] Note that the results in table 1 seem to indicate that the Γ points give low spring constants relative to the S and T points, and that the larger unit cell gives stiffer spring constants.
[28] The ratio of displacements near a vacancy and the displacements in a perfect crystal under uniform external stress are considered in [23]. Using a valence force potential, they report a ratio of 11 ± 1. Note that in [4], these numbers are referred to as calculated for uniaxial stress.
[29] We calculate these values from figure 1(*c*) in [10]. They define their displacement coordinate in terms of the displacements found in [30]. Note that there are two such displacements, and Dr Lipari tells us that it is the smaller displacement of 0.24 Å that was used. [9] erroneously refers to the V_Θ of the values of Lipari *et al* as 40% smaller than theirs.
[30] Watkins G D 1975 *Lattice Defects in Semiconductors 1974 (Inst. Phys. Conf. Ser. 23)* ed F A Huntley (London: Institute of Physics) p 1
[31] Jaros M, Rodriquez C O and Brand S 1979 *Phys. Rev.* B 19 3137
[32] This inward relaxation is analogous to the behaviour of the ammonia molecule, in which the filled lone-pair orbitals repel the N–H bonds, decreasing the bond angles from tetrahedral values. The filled lone pairs of the Si vacancy repel the Si–Si back bonds and as a result B decreases (this is called the VSEPR model, see Gillespie R J and Nyholm R S 1957 *Quart. Rev. Chem. Soc.* 11 239). Our result is qualitatively similar to that of [20], where the authors find a relative inward breathing distortion of 0.20 Å for the neutral vacancy as compared to the doubly positive state; and to the result of [24] where the corresponding relaxation is 0.03 Å.
[33] In [11] we find the inconsistent results for V_Θ of -0.5 eV Å^{-1} in the text and -4 eV Å^{-1} in figure 14.
[34] Our reading off from figures 15 and 16 in [31] gives inconsistent results for V_Θ (-0.3 and -8 eV Å^{-1}, respectively). It is stated in [9] that the values of [31] are considerably smaller than the values of [10].
[35] Lidiard A B and Stoneham A M 1967 *Sci. Technol. Indust. Diamonds* 1 1
[36] Note that the derivative of the V_Θ result from the $\Gamma(32)$ point is somewhat smaller, consistent with the lower degree of localization of the t_2 states. Thus we found earlier that at the $\Gamma(32)$ point there is 30% less charge on the vacancy nearest neighbours than for the S(32) point. This effect is real and should be seen experimentally whenever a JT distorted electronic state is near the band edges. It is consistent with the lower V_Θ found in [9] for negative as opposed to positive distortions along the Θ coordinate, since for the negative distortions the B_2 state moved to the edge of the conduction band.
[37] It is noted in [9] that their V_Θ was quantitatively sensitive to the degree of completeness of their Green function and that for the lower cutoff used, the result was about 30% smaller. Other sources of errors present in their calculation were the pseudopotentials used, the slight adjustment of the potentials performed to correct the bandgap and the lack of relaxations. We tested our calculation by increasing the cutoff energy from 7 to 11 Ryd and found that at $B = 2.17$ Å V_Θ decreased by only 12%. We further investigated whether or not including relaxations beyond the four nearest neighbours (that we included, but [9] did not in the calculation of the electronic states) would change our V_Θ. We found that at $B = 2.45$ Å for a distortion of 0.27 Å in normal coordinates the freezing of the atoms further away in their breathing-mode relaxed positions increased V_Θ by only 9%; while at $B = 2.17$ Å and freezing the atoms in their bulk positions the effect was to increase V_Θ by only 3% (there was a large 0.13 eV shift down in the centre of mass of the t_2 states). Finally, the supercell correction from section 4 only contributes 0.12 eV Å^{-1} for $B = 2.35$ Å.
[38] Stich I, Payne M C, King-Smith R D, Lin J-S and Clarke L J 1992 *Phys. Rev. Lett.* 68 1351
Brommer K D, Needels M, Larson B E and Joannopoulos J D 1992 *Phys. Rev. Lett.* 68 1355
[39] Larkins F P and Stoneham A M 1971 *J. Phys. C: Solid State Phys.* 4 154
[40] There are three t_2 representations, two of which correspond to an overall translation and an overall rotation. The two quoted modes came from a vibrational analysis and presumably include the

overall translation or rotation. G Baraff 1992 private communication.

[41] The strong dependence of U_{JT} on B, coupled with the controversial size of the B distortion (see section 3) suggests that the effective electronic correlation energy is yet to be accurately calculated. Note however, that present estimates are in excellent agreement with experiment: theory predicted $U = -0.13$ eV [9] and experiment measured $U = -0.08$ eV [3].

[42] Yin M T and Cohen M L 1982 *Phys. Rev.* B **26** 5668

[43] This is contrary to what is stated in [4] and [9], which say that the (-2) charge state is similar to the (-1) state and undergoes a further trigonal distortion.

[44] This argument is at odds with [9], which states that the high-occupancy states have 'insufficient Jahn–Teller lowering, as we approach the fully occupied multiplet'.

[45] For a discussion of the sizes of substitutional vacancy-like impurities in Si, see Tarnow E 1992 *Europhys. Lett.* **17** 157

[46] Humphreys R G, Brand S and Javros M 1983 *J. Phys. C: Solid State Phys.* **16** L337